

Mutation rules and the evolution of Sparseness and Modularity in Biological Systems

Tamar Friedlander¹, Avraham E. Mayo¹, Tsvi Tlusty^{2,3} and Uri Alon^{1,*},

¹Department of Molecular Cell Biology

²Department of Physics of Complex Systems

Weizmann Institute of Science

Rehovot 76100, Israel

³Simons Center for Systems Biology,

Institute for Advanced Study,

Princeton NJ 08540, USA.

* uri.alon@weizmann.ac.il

Classification: Biological Sciences: Systems Biology

Short title: Mutation-rules and the evolution of Modularity

Abstract

Biological systems show two structural features on many levels of organization: sparseness, in which only a small fraction of possible interactions between components actually occur; and modularity – the near decomposability of the system into modules with distinct functionality. Recent work suggests that modularity can evolve in a variety of circumstances, including goals that vary in time such that they share the same subgoals (modularly varying goals). Here, we studied the origin of modularity and sparseness focusing on the nature of the mutation process, rather than variations in the goal. We use simulations of evolution with different mutation rules. We find that commonly used sum-rule mutations, in which interactions are mutated by adding random numbers, do not lead to modularity or sparseness except for special situations. In contrast, product-rule mutations in which interactions are mutated by multiplying by random numbers— a better model for the effects of biological mutations – lead to sparseness naturally. When the goals of evolution are modular, in the sense that specific groups of inputs affect specific groups of outputs, product-rule mutations lead to modular structure; sum-rule mutations do not. Product-rule mutations generate sparseness and modularity because they keep small interaction terms small.

Introduction

Biological systems show certain structural features on many levels of organization. Two such features are sparseness and modularity. Sparseness means that most possible interactions between pairs of components are not found. For example, less than 1% of the possible interactions are found in gene regulation networks of bacteria and yeast (1). The second feature, modularity, is the near-decomposability of a system into modules - sets of components with many strong interactions within the set, and few significant interactions with other sets. Each module typically performs a specific biological function. Modularity is found for example in protein structure (functional domains), in regulatory networks (gene modules, network motifs), and in body plans (organs, systems) - for reviews see (2–5). While modular networks are essentially sparse, the opposite is not true. Even if interactions are few, they could be evenly distributed and therefore not form modules.

To understand the origin of these structural features, computer simulations of evolution are used. These simulations begin with a set of structures, mutate the elements of the structures, evaluate fitness of each structure according to a given goal, and then select the highest fitness structures. The most commonly used form of mutation in these simulations is sum-rule mutation: adding to the value of each element a random number. Such simulations typically find optimal structures which satisfy the goal. However, they generally do not yield modular or sparse structure. Even if one starts with a modular solution, these simulations typically drift towards non-modular solutions, which are usually much more prevalent and sometimes perform better given the goal (6). This leaves open the question of how and why sparseness and modularity evolve in biology.

Several studies have addressed this question employing different approaches. For example, neutral models suggest that duplicating parts of a network can increase its modularity (“duplication-differentiation” model (7)) or similarly that mutation, duplication and genetic drift (8) can lead to modularity. On the other hand, other studies suggest that modularity can be selected for, either indirectly or directly. Modularity has been suggested to be beneficial because it provides robustness to mutations (9), improves the ability to accommodate beneficial foreign DNA (10), breaks developmental constraints (11), evolves due to selection for environmental robustness (12, 13) or because the same network has to support multiple expression patterns (14). Kashtan *et al.* (15–17) found that when goals change with time, such that goals are made of the same set of subgoals in different combinations - a situation termed modularly varying goals - the system can evolve modular structure. Each module in the evolved structure solves one of the subgoals, and modules are quickly rewired when the goal changes. Modularly varying goals was tested in several model systems, showed modularity under a range of parameters (but not for all parameters) and used sum-rule mutations when applicable. Modularly varying goals also speed up evolution relative to unchanging goals (18), a phenomenon analyzed using analytically solvable models (6). Many of the aforementioned models apply only to a range of parameters and scales of organization; thus, additional mechanisms are needed to explain the origin of modular structure in biology.

Here, we address the role of the mutation rule on the evolution of modularity and sparseness. Most studies that use simulations to study evolution employ a simple rule to specify how mutations change the parameters in the structure that is evolved - namely the 'sum rule', in which a parameter is mutated by adding a random number drawn from a specified distribution. Here, we note that this sum rule is usually not a good description of biological mutations. Instead they are better approximated by product-rule processes. For example, the effect of cumulative mutations on an enzyme's activity is found to be multiplicative (19). Similarly, the effect of mutation on binding of proteins to DNA is thought to be multiplicative to a first approximation (20, 21), such that the change in affinity caused by several mutations is approximately the product of the effects of each mutation.

One fundamental reason for the product rule is that mutations affect molecular interactions such as hydrogen bonds. This affects the free energy in an approximately additive way, assuming that the different molecular interactions are independent to a first approximation. Since affinity and reaction rate are exponential in free energy, the effects of cumulative mutations are approximately multiplicative. Note that in population genetics, there are different meanings to 'additive' and 'multiplicative' mutations (22), and thus we chose the terms 'sum-rule' and 'product-rule' to avoid confusion.

A related feature of mutations is that they more often reduce the absolute strength of the interaction or activity than increase it (23, 24). This asymmetry can be captured using product-rule mutations: for example, multiplying by a random number normally distributed $\mathcal{N}(\tilde{1}, \sigma)$ gives equal probability to multiply by 0.5 or 1.5, which tends to reduce the absolute size of the element because in order to revert a 0.5-mutation, one needs to multiply by a 2-mutation, which is less likely to occur.

To study the role of product-rule mutations, we compare evolution of simple model structures under sum-rule and product-rule mutations in computer evolution simulations. This is of interest because most simulations of evolution used sum-rules for mutations. We find that product-rule mutations lead to evolution of sparseness without compromising fitness. This relates to the study of Burda *et al.* which used a mutation rule that is approximately product-rule (25). In contrast, sum-rule mutations only lead to sparseness in special conditions, such as when the model parameters are constrained to be non-negative. Furthermore, when the goal is modular, we find that product-rule mutations lead to modular structures, whereas sum-rule mutations generally do not. Unlike Kashtan *et al.*, (6, 15, 16) here modularity arises from modular goals without need to change goals over time. We study the speed and scaling laws of this process. The basic reason that product-rule mutations lead to sparseness and modularity is that they keep small interaction terms small and thus cause the evolutionary dynamics to approach structures that have optimal fitness with minimal number of interactions.

Results

A simple nonlinear model of transcription networks

To study the effect of the mutation rule on evolved structure, we use a standard evolutionary simulation framework (26, 27). Briefly, the evolutionary simulation starts with a population of N structures, duplicates them, and mutates each structure with some probability according to a mutation rule (the mutation rules described below will be our main focus). Fitness is evaluated for each structure in comparison to a goal. The fittest individuals are selected by a selection criterion, and the process is repeated, until high fitness evolves (Fig. 1A).

We consider, for simplicity, structures described by continuous-valued matrices. These serve as simple models for biological interactions, where the elements of the matrix A_{ij} are the interaction strengths between components i and j in the system. Evolution entails varying the matrix elements to reach defined goals. We previously used a linear model to study evolution (6, 28), in which we evolved the matrix A to satisfy the goal $Au = v$, where u and v are vectors. The fitness is the distance to the goal, $F = -\|Au - v\|$ where $\|\cdot\|$ denotes sum of squares of elements (related to Fisher's geometric model (29)).

This matrix model is linear, whereas most biological systems are not. To make a simple nonlinear model, we introduce a matrix multiplication model in which we evolve two matrices A and B towards the goal $AB = G$, where G is a specified matrix (Fig. 1B). The fitness in this case is $F = -\|AB - G\|$. Note that there is an infinite number of matrix pairs A and B that satisfy a given goal G .

The model can be interpreted with biological meaning using a transcription network as an example: If A is the matrix connecting transcription factor (TF) activities to gene expression, the relationship $Au = v$ means that a vector of TF activities u leads to a vector of gene expression, v . Similarly, if B is a matrix of interactions between external signals s and TF activities, one finds that the TF activities are $u = Bs$. Thus, the output gene expression vector that results from an input vector of signals s is ABs . The goal $AB = G$ means that for every set of signals s , the gene expression at the output of the system is $ABs = Gs$, where Gs is the desired gene response.

Product-rule mutations lead to sparse structures, sum-rule mutations do not

We compared sum and product mutation rules in evolving the model systems using an evolutionary simulation. The sum-rule is the commonly used addition of a normally distributed random number to a randomly chosen element of the matrices,

$$\text{Sum-rule} \quad A_{ij} \rightarrow A_{ij} + \mathcal{N}(0, \sigma) \text{ or } B_{ij} \rightarrow B_{ij} + \mathcal{N}(0, \sigma).$$

We also tested product-rules, in which an element of the matrix is multiplied by a random number. We tested

$$\text{Product-rule} \quad A_{ij} \rightarrow A_{ij} \cdot \mathcal{N}(\mu, \sigma) \text{ or } B_{ij} \rightarrow B_{ij} \cdot \mathcal{N}(\mu, \sigma).$$

We study the case of $\mu = 1$, and also cases in which $\mu < 1$ and $\mu > 1$. We also tested symmetric multiplication rules where the random number is log-normally distributed around a mean $\mu = 1$, and thus has equal chance to increase or decrease the absolute strength of the interaction.

Symmetric product-rule $A_{ij} \rightarrow A_{ij} \cdot \mathcal{LN}(\mu, \sigma)$ or $B_{ij} \rightarrow B_{ij} \cdot \mathcal{LN}(\mu, \sigma)$.

All cases gave qualitatively similar results, and most of the data below is for multiplying by $\mathcal{N}(1, \sigma)$. We also tested other forms of mutation distributions, including long tailed distributions that describe experimental data on mutation sizes [Gamma distributions, (24)], and found that the results are insensitive to the type of distribution used. Similarly, we tested the effect of mutation size, that is the parameter σ , which we varied between 0.01 and 3, and find that the results are insensitive to this parameter. The evolutionary simulation and parameters are described in the Methods section below.

To demonstrate the effect of the mutation rule, we begin with a very simple model, namely a structure with two elements, x and y , with fitness $F = -(x + y - 1)^2$. The optimal solutions lie on a line in the (x, y) plane, namely $x + y = 1$ (Fig. 2A). Evolutionary simulations reach this line regardless of the mutation rule. Populations under sum-rule mutations evolve and spread out over the line. Over time the population slowly diffuses along the line of optimal fitness. In contrast, product-rule mutations lead to solutions near the axes, either $(x = 0, y = 1)$, or $(x = 1, y = 0)$. In other words, they lead to solutions in which one of the elements is close to zero – these are the sparsest solutions that satisfy the goal.

The intuitive reason for the sparseness achieved by product-rule mutations is that once they are near a zero element, the effective diffusion rate decreases. Strictly zero terms are fixed-points and near-zero terms remain small under mutations - so that the population becomes concentrated near zero elements. Sum-rule mutations, in contrast, show a constant drift rate regardless of the value of the elements. A full analytical solution of the dynamics of this simple model can be obtained by means Fokker-Planck equations (SI Appendix, section 1), in excellent agreement with the simulations.

We tested product-rule mutations in the nonlinear matrix-multiplication model, using as goals full rank matrices G . In numerical simulations, we refer to terms that are relatively small (<0.1% of the average element in G) as “zero terms”, because strictly zero terms are not reached in finite time. We find that product-rule mutations lead to sparseness: matrices A and B with the highest number of zeros possible while still satisfying the goal. In contrast, sum-rule mutations result in non-sparse solutions A and B with non-zero elements (Fig. 3).

The sparse solutions found with product-rule mutations have many zero terms, whose number can be computed by means of the LU decomposition theorem of linear algebra. The LU decomposition expresses a nonsingular matrix as a product of an upper triangular matrix and a lower triangular matrix (30)). The total number of zeros in A and B is the number of zero elements in the LU decomposition of G . This number can be calculated exactly: for a given full

rank matrix G of dimension D with no zero elements, the maximal number of zeros in A and B together is $D^2 - D$ (for proof see SI Appendix). This result is found in our simulations.

The zeros are distributed between A and B in different ways in different simulations: Sometimes A and B are both (upper and lower) triangular, each with $(D^2 - D)/2$ zero elements. Other runs show one full matrix with no zeros and the other a diagonal matrix with $D^2 - D$ zeros. All other distributions of zeros are also found (Fig. 2B). When G is full rank and has k zeros, the total number of zeros in the evolved matrices A and B is $D^2 - D + k$, again the maximal possible number of zeros in matrices that show optimal fitness (for proof see SI Appendix).

We note that there is a special situation in which sum-rule mutations can also lead to sparseness in the present models. This occurs when the models are constrained to have only non-negative terms $A_{ij}, B_{ij} \geq 0$. In this case, the sum rule, constrained to keep terms non-negative – for example, by using $A_{ij} \rightarrow \max(0, A_{ij} + \mathcal{N}(0, \sigma))$, can also lead to sparseness. This relates to known results from non-negative matrix factorization (31). However, in general biological models, structural terms are expected to be both negative and positive, representing, for example, inhibition and activation interactions between components.

When the goal is modular, product-rule mutations lead to modular structure, sum-rule mutations do not

Up to now, we considered goals G which are described by general matrices. We next limit ourselves to the case where the goals G are described by matrices which are modular, for example, diagonal or block diagonal matrices. The main result is that when the goals are modular, the evolved structures A and B are also modular if mutations are product-rule; in contrast, with sum-rule mutations A and B are not modular even though the goal is modular.

We first define modular structures and modular goals in the context of the present study. Modular structures are structures that can be decomposed into sets of components, where each set shows strong interactions within the set and weak interactions with other sets (2, 3, 32, 33) (Fig. 1B). Here, modular structure means block-diagonal matrices. For ease of presentation, we first consider the most modular of structures – namely diagonal matrices. We define modularity by $M = 1 - \langle |n| \rangle / \langle |d| \rangle$ where $\langle |n| \rangle$ and $\langle |d| \rangle$ are the mean absolute value of the non-diagonal and diagonal terms respectively, and where we permute rows/columns to maximize modularity M (same permutation for rows of A and columns of B , see SI Appendix). Thus, $0 \leq M \leq 1$: a diagonal matrix has $M = 1$, and a matrix with large non-diagonal terms has low M .

Modular goals are goals which can be satisfied by a modular structure. Modular goals are represented by diagonal or block-diagonal goal matrices G . These goals, in the biological interpretation of transcription networks (Fig. 1B), are goals in which each small set of signals

affects a distinct set of genes, and not the rest of the genes. For example, the signal lactose affects the *lac* genes in *E. coli*, whereas a DNA damage signal affects the *SOS* DNA-repair genes, with little crosstalk between these sets. We believe that modular goals are the norm in biology.

We note that a modular goal does not necessarily lead to modular structures. For example the goal $G = I$ is modular since I is the diagonal identity matrix. This modular goal can be satisfied by a product of infinitely many pairs of non-modular matrices AB . In fact, for every invertible A , the inverse $B = A^{-1}$ satisfies the goal. As a result, the vast majority of the possible solutions are non-modular (modular solutions have measure zero among possible solutions to $AB = G$). In line with this observation, we find that simulations with sum-rule mutations lead to solutions with optimal fitness ($AB = G$), but with non-modular structure A and B (Fig. 3).

In contrast, we find that product-rule mutations lead to modular structures A and B , for a wide range of parameters. For the goal $G = I$, the evolved A and B are both diagonal matrices, with elements on the diagonal of A that are the inverse of the corresponding elements on the diagonal of B . Thus $AB = G$. Similar results are found if the goal is nearly modular (e.g. diagonal with small but nonzero non-diagonal terms): in this case, the evolved A and B are both nearly diagonal (Fig. S10).

We also studied block-modular goals. In this case, product-rule mutations led to block-modular matrices A and B , with the same block structure as the goal matrix G (Fig. 2C). Each of the blocks in the matrices A and B had the maximal number of zeros possible so that the product of the two blocks is equal to the corresponding block in the goal matrix G (the total number of zeros is equal to that in the LU decomposition of each block).

It is important to note that in order to observe the evolution of modularity in the present setting, one needs to have selection criteria which are not too strict, otherwise non-modular solutions cannot be escaped effectively (SI Appendix). In other words, overly strict selection does not allow the search in parameter space needed for product-rule mutations to reach near-zero elements. In the present simulations, we find evolution of modularity using standard selection methods including tournament, elite (truncation) and continuous Boltzmann-like selection (see Methods, and SI Appendix for analysis of sensitivity to parameters).

Time to evolve modular structure increases polynomially with dimension

We studied the dynamics of the evolutionary process in our simulations with product-rule mutations. We find that over time, fitness and modularity both generally increase, until a solution with optimal fitness and maximal modularity is achieved. We find that the nonlinear model often shows plateaus where fitness is nearly constant, followed by a series of events in which fitness improves sharply (Fig. 4) (12, 34). In these events, modularity drops momentarily. Analysis shows that the plateaus represent non-modular and sub-optimal structures. A mutation

occurs which reduces modularity but allows the system to readjust towards higher fitness, and then to regenerate modularity.

We also tested the time to reach high fitness solutions, and its dependence on the dimension of the matrices D . The time to high fitness solutions depends on the settings of the simulations: initial conditions, selection criteria and mutation rates and size, and the stopping criteria of the simulations. Here we present results in which time to high fitness was measured as the median time over repeat simulations to reach within 0.01 of optimal fitness, with mutation size ($\cdot\mathcal{N}(1,0.1)$) and probability of mutation per element that is dimension-independent ($p = 5 \times 10^{-4}$). Initial conditions were matrices with small random elements ($\mathcal{U}(0,0.05)$). The time to high fitness increased approximately as D^{θ_1} with $\theta_1 = 1.41$ [1.40, 1.42] [confidence intervals 5%, 95%] and the time to modularity (see Methods for definition) increased as D^{θ_2} with $\theta_2 = 1.2$ [1.16, 1.23] [confidence intervals 5%, 95%] (Fig. 5).

Discussion

We find that product-rule mutations lead evolution towards structures with the maximal number of zeros (or very small interaction terms) that satisfy the fitness objective. Thus, product-rule mutations lead to sparseness. When the goal is modular, product-rule mutations lead to modular structure. This is in contrast to sum-rule mutations, which lead, under the same conditions, to non-sparse and non-modular solutions.

The mechanism by which product-rule mutations lead to sparseness and modularity is that near-zero interaction terms are kept small by product-rule (but not sum-rule) mutations. A second effect is mutation asymmetry, where it is more likely to reduce an interaction than increase it. However, using a symmetric product-rule (multiplying by a number drawn from a log-normal distribution) still leads to sparseness and modularity. Thus, the asymmetry effect is not essential for the present conclusions. Furthermore, in special situations a sum-rule can also lead to sparseness, namely if the structural terms in the model are constrained to be non-negative.

The present mechanism does not exclude previous mechanisms for the evolution of modularity. In fact, it can work together with previous mechanisms and enhance them. For example, in Kashtan *et al.* (6, 15, 17, 18), modularity evolved when the modular goal changed over time. In the present study, no change of the goal over time is required. Using product-rule mutations in the models of Kashtan *et al.* (instead of the original sum-rule mutations) may enhance the range of parameters over which modularity evolves. Another difference from some previous studies is that modularity evolves here with no need for an explicit cost for interaction terms in the fitness function (6, 15, 17, 18, 35). Adding such a cost would likely enhance the evolution of modularity.

Product-rule mutations are more realistic than sum-rule mutations, because of the nature of biological interactions. Further studies can use more microscopic models for

mutations (such as Ising-like models for bonds between macromolecules (25, 36)), and explore the effect of mutations that set interactions to near-zero with large probability. Due to the inherent product-rule nature of biological mutations, we could not think of experimental tests that can compare sum-rule to product-rule mutations, beyond computer simulations or experiments in the realm of electronics (37, 38) or mechanics (39).

The present mechanism for modularity can exist together with other mechanisms (2, 3), and potentially to enhance them. Such mechanisms can help explain the origins of modularity in biology.

Materials and Methods:

Evolutionary simulation

Here we detail our evolutionary computer simulation. Simulation was written in Matlab using standard framework (26, 27) in order to test our model. We initialized the population of matrix pairs by drawing their $N \cdot 2D^2$ terms from a uniform distribution. Population size was set as $N = 500$.

At each generation the population was duplicated. One of the copies was kept unchanged, and elements of the other copy had a probability p to be mutated – as we explain below. Fitness of all $2N$ individuals was evaluated by $F = -||AB - G||$, where $|| \cdot ||$ denotes the sum of squares of elements (29). The best possible fitness here is zero, achieved if $AB = G$ exactly. Otherwise, fitness values are negative. In the figures we usually show the absolute value of mean population fitness. The goal matrix was either diagonal $G = 2 \times I$, nearly-diagonal (diagonal matrix with small non-diagonal terms), block-diagonal or full rank with no zero elements. N individuals were then selected out of the $2N$ population of original and mutated ones, based on their fitness. This mutation–selection process was repeated again and again until the simulation stopping condition was satisfied (usually when mean population fitness was less than 0.01 from the optimum).

Mutation: We tested point mutations in our simulation assuming statistical independence between mutations at different elements. We set mutation rate such that on average 10% of the population members were mutated at each generation, so the element-wise mutation rate was $\sim \frac{0.1}{2D^2}$. This relatively low mutation rate enables beneficial mutants to reproduce on average at least 10 times before they are mutated again. In simulations where we compared dependence on matrix dimension (Fig. 5) we used the same mutation rate at all dimensions, generally the one that pertains to the highest dimension used in the simulation.

We randomly picked the matrix elements (in both A and B) that would be mutated. Mutation values were drawn from a Gaussian distribution. For sum-rule mutations, this random number was added to the mutated matrix value: $A_{ij} \rightarrow A_{ij} + \mathcal{N}(0, \sigma)$ or $B_{ij} \rightarrow B_{ij} + \mathcal{N}(0, \sigma)$, and for

product-rule mutation, the mutated matrix element was multiplied by the random number: $A_{ij} \rightarrow A_{ij} \cdot \mathcal{N}(\mu, \sigma)$ or $B_{ij} \rightarrow B_{ij} \cdot \mathcal{N}(\mu, \sigma)$. Mean mutation value μ was usually taken as 1, however we also tested other values of μ (both larger and smaller than 1) and results remained qualitatively similar, only the time-scales changed. In most simulations shown here we used $\sigma = 0.1$ (unless stated otherwise). Fitness convergence and its time scale depend on the mutation frequency and size, as demonstrated in our sensitivity test (SI Appendix).

Selection methods: We tested 3 different selection methods, all gave qualitatively very similar results with only difference in time scales. Most results presented here were obtained with tournament selection (see (27) chap. 9). We also tested “truncation-selection” (“elitism”) and proportionate reproduction with Boltzmann-like scaling. For a detailed description see SI Appendix.

Definition of modularity: if the goal is diagonal, we define modularity as $M = 1 - \langle |n| \rangle / \langle |d| \rangle$ where $\langle |n| \rangle$ and $\langle |d| \rangle$ are the mean absolute value of the non-diagonal and diagonal terms respectively. At each generation, the D largest elements of each matrix (both A and B), were considered as the diagonal $\langle |d| \rangle$ and the rest $D^2 - D$ terms as the non-diagonal ones $\langle |n| \rangle$. Averages were taken over matrix elements and over the population. This technique copes with the unknown location of the dominant terms in the matrices, which could form any permutation of a diagonal matrix. Thus, $0 \leq M \leq 1$: a diagonal matrix has $M = 1$, and a matrix whose terms are all equal has $M = 0$. Since we choose the largest elements to form the diagonal, negative values of M are not allowed. When the goal is non-diagonal, one can use standard measures for modularity such as (33).

Calculation of time to modular structure: To estimate the time when modular structure is first obtained, we used the following approximation for fitness value with diagonal goal. Assume that A and B are D -dimensional matrices consisting of 2 types of terms: diagonal terms all with size d and non-diagonal terms all with size n and that the goal is $G = g \times I_{D \times D}$. The fitness then equals:

$$-F = D[d^2 + (D - 1)n^2 - g]^2 + D(D - 1)(2dn + (D - 2)n^2)^2.$$

We collect terms by powers of n , and obtain a constant term and terms with powers $n^{2,3,4}$. Modular structure is obtained when the solution has the correct number of dominant terms at the right location and their size is approximately $d^2 \cong g$. At the beginning of the temporal trajectory, when non-diagonal elements are relatively large, F is dominated by the $O(n^4)$ term. When a modular structure emerges, non-diagonal elements become relatively small, and the dominant term remaining in F is $O(n^2)$. Our criterion for determining time to modular structure was the time when the $O(n^2)$ term first became dominant, i.e. when $F - n^2(\dots) < n^2(\dots)$.

Acknowledgements

The research leading to these results has received funding from the Israel Science Foundation and the European Research Council under the European Union's Seventh Framework

Programme (FP7/2007-2013) /ERC Grant agreement n° 249919. U. A. is the incumbent of the Abisch-Frenkel Professorial Chair. T.F. acknowledges a Clore fellowship. We thank Yuval Hart, Adam Lampert, Omer Ramote, Hila Sheftel, Oren Shoval and Pablo Szekely for critical reading of the manuscript; Amos Tanay and Dan Tawfik for useful discussions.

References

1. Gama-Castro S et al. (2011) RegulonDB version 7.0: transcriptional regulation of Escherichia coli K-12 integrated within genetic sensory response units (Gensor Units). *Nucleic Acids Research* 39:D98–D105.
2. Lorenz DM, Jeng A, Deem MW (2011) The emergence of modularity in biological systems. *Physics of Life Reviews* 8:129–160.
3. Wagner GP, Pavlicev M, Cheverud JM (2007) The road to modularity. *Nature Reviews Genetics* 8:921–931.
4. Hartwell LH, Hopfield JJ, Leibler S, Murray AW, others (1999) From molecular to modular cell biology. *Nature* 402:47.
5. Alon U (2003) Biological networks: the tinkerer as an engineer. *Science* 301:1866–1867.
6. Kashtan N, Mayo AE, Kalisky T, Alon U (2009) An Analytically Solvable Model for Rapid Evolution of Modular Structure. *PLoS Comput Biol* 5:e1000355.
7. Solé RV, Valverde S (2008) Spontaneous Emergence of Modularity in Cellular Networks. *J R Soc Interface* 5:129–133.
8. Force A et al. (2005) The origin of subfunctions and modular gene regulation. *Genetics* 170:433–446.
9. Variano EA, McCoy JH, Lipson H (2004) Networks, dynamics, and modularity. *Physical review letters* 92:188701.
10. Rainey PB, Cooper TF (2004) Evolution of bacterial diversity and the origins of modularity. *Research in microbiology* 155:370–375.
11. Leroi AM (2000) The scale independence of evolution. *Evolution & development* 2:67–77.
12. Ancel LW, Fontana W, others (2000) Plasticity, evolvability, and modularity in RNA. *Journal of Experimental Zoology* 288:242–283.
13. He J, Sun J, Deem MW (2009) Spontaneous emergence of modularity in a model of evolving individuals and in real networks. *Phys Rev E* 79:031907.
14. Espinosa-Soto C, Wagner A (2010) Specialization Can Drive the Evolution of Modularity. *PLoS Comput Biol* 6:e1000719.

15. Kashtan N, Alon U (2005) Spontaneous Evolution of Modularity and Network Motifs. *PNAS* 102:13773–13778.
16. Parter M, Kashtan N, Alon U (2008) Facilitated variation: How evolution learns from past environments to generalize to new environments. *PLoS Computational Biology* 4:e1000206.
17. Kashtan N, Parter M, Dekel E, Mayo AE, Alon U (2009) Extinctions in heterogeneous environments and the evolution of modularity. *Evolution* 63:1964–1975.
18. Kashtan N, Noor E, Alon U (2007) Varying environments can speed up evolution. *Proceedings of the National Academy of Sciences* 104:13711.
19. Wells JA (1990) Additivity of mutational effects in proteins. *Biochemistry* 29:8509–8517.
20. Maerkl SJ, Quake SR (2007) A Systems Approach to Measuring the Binding Energy Landscapes of Transcription Factors. *Science* 315:233–237.
21. Von Hippel PH, Berg OG (1986) On the specificity of DNA-protein interactions. *Proceedings of the National Academy of Sciences* 83:1608.
22. Wacholder S, Han SS, Weinberg CR (2011) Inference from a multiplicative model of joint genetic effects for ovarian cancer risk. *Journal of the National Cancer Institute* 103:82–83.
23. Soskine M, Tawfik DS (2010) Mutational effects and the evolution of new protein functions. *Nature Reviews Genetics* 11:572–582.
24. Silander OK, Tenaillon O, Chao L (2007) Understanding the evolutionary fate of finite populations: the dynamics of mutational effects. *PLoS biology* 5:e94.
25. Burda Z, Krzywicki A, Martin OC, Zagorski M (2010) Distribution of essential interactions in model gene regulatory networks under mutation-selection balance. *Phys Rev E* 82:011908.
26. Goldberg DE (1989) *Genetic Algorithms in Search, Optimization, and Machine Learning* (Addison-Wesley).
27. Spall JC (2003) *Introduction to Stochastic Search and Optimization: Estimation, Simulation and Control* (Wiley-Blackwell).
28. Lipson H, Pollack JB, Suh NP (2007) On the origin of modular variation. *Evolution* 56:1549–1556.
29. Fisher RA (1930) *The Genetical Theory of Natural Selection* ed Bennett JH (Oxford University Press, USA). 1st Ed.
30. Cormen TH, Leiserson CE, Rivest RL, Stein C (2001) *Introduction To Algorithms* (MIT Press).
31. Lee DD, Seung HS (1999) Learning the parts of objects by non-negative matrix factorization. *Nature* 401:788–791.

32. Simon HA (1962) The architecture of complexity. *Proceedings of the American philosophical society* 106:467–482.
33. Newman MEJ (2006) Modularity and community structure in networks. *Proceedings of the National Academy of Sciences* 103:8577–8582.
34. Kauffman S, Levin S (1987) Towards a general theory of adaptive walks on rugged landscapes. *Journal of Theoretical Biology* 128:11–45.
35. Pan RK, Sinha S (2007) Modular networks emerge from multiconstraint optimization. *Phys Rev E* 76:045103.
36. Lancet D, Sadovsky E, Seidemann E (1993) Probability Model for Molecular Recognition in Biological Receptor Repertoires: Significance to the Olfactory System. *PNAS* 90:3715–3719.
37. Thompson A, Harvey I, Husbands P (1996) in *Towards Evolvable Hardware*, Lecture Notes in Computer Science., eds Sanchez E, Tomassini M (Springer Berlin / Heidelberg), pp 136–165. Available at: <http://www.springerlink.com/content/f6m8731w5706w108/abstract/>.
38. Thompson A (1997) in *Evolvable Systems: From Biology to Hardware*, Lecture Notes in Computer Science., eds Higuchi T, Iwata M, Liu W (Springer Berlin / Heidelberg), pp 390–405. Available at: <http://www.springerlink.com/content/u734gr0822r13752/abstract/>.
39. Zykov V, Mytilinaios E, Adams B, Lipson H (2005) Robotics: Self-reproducing machines. *Nature* 435:163–164.

Figure Captions

Fig. 1 – Evolutionary simulation scheme, and definition of model. **(A)** Simulation was initiated by randomly choosing N population members each consisting of 2 matrices A and B . The next steps were repeated at each generation until the stopping condition was satisfied: the population was duplicated, one copy was kept unchanged and the other was mutated with probability p . Mutation could be either sum-rule or product-rule. Fitness of all $2N$ members (original and mutated) was evaluated by the distance of the product AB from a desired goal matrix G , $F = -\|AB - G\|$, where $\|\cdot\|$ denotes the square of the L_2 (Frobenius) norm (sum of squares of terms). N individuals were selected according to their fitness. Several selection methods were employed (see SI Appendix for details). The simulation was stopped when the mean population fitness reached a value which was within a preset difference from the optimal fitness (usually 0.01). **(B)** Model represents a three layer network with a linear transformation function. Input signals s are transformed to intermediate layer activities (transcription factors) u with $u = Bs$. The intermediate layer is then transformed to output layer (gene expression) $v = Au = ABs$. Modularity means block or diagonal structure of the matrices, corresponding to signals that affect only subsets of intermediate and output nodes.

Fig. 2 – Product-rule mutations reach sparse solutions, sum-rule ones do not. (A) We demonstrate the difference between sum-rule and product-rule mutations in a simple 2–variable system (x, y) , where the goal is that $x + y = 1$. The optimal solutions lie on the line $y = 1 - x$. We compare solutions to this problem achieved by 3 different mutational schemes. Sum-rule mutations ($+\mathcal{N}(0,0.5)$ red circles) provide solutions that are spread along the line. In contrast, solutions achieved with both Gaussian product-rule ($x \mathcal{N}(1,0.5)$ blue diamonds) and log-normal product-rule ($x \mathcal{L}\mathcal{N}(1,0.5)$) green squares) are concentrated near the intersection with the axes, i.e. near either $(0,1)$ or $(1,0)$. Since one coordinate is near zero, these are sparse solutions. Inset illustrates the solutions obtained with Gaussian product-rule mutations, demonstrating that matrix values can be negative as well as positive. Evolutionary simulation parameters were $p=0.5$, $N=500$, selection scheme was Boltzmann-like selection with $\beta=10$. Simulations initiated utilizing random matrices with elements $\mathcal{U}(0,0.05)$. **(B)** Sparse solutions evolve in the nonlinear model under product-rule mutations in response to a full (non-zero) goal matrix G . The solutions have the maximal number of zeros while still satisfying the goal. Zeros are distributed between the two matrices A and B . Shown are the possible configurations of A and B for matrices of dimension $D = 3$, in which 6 zeros are distributed between the two matrices A and B . **(C)** In general, if the goal is block diagonal, each of its blocks can be decomposed separately into blocks of A and B , such that each block has the maximal number of zeros possible. Here we show an example in $D = 4$, where G has 2 blocks of 2×2 . The evolved A and B are such that each of their blocks is either an upper or a lower triangular matrix. Color represents numerical value (white = zero).

Fig. 3 – Product-rule mutations lead to modular structure under modular goal, sum-rule mutations do not. (A) Both sum-rule and product-rule mutations reach high fitness towards the goal $G = 2I$. **(B)** Product-rule mutations reach high modularity, but sum-rule mutations do not. Simulations are in the nonlinear model, matrix dimension $D = 4$. Examples of matrices drawn from the simulations are shown, with gray scale corresponding to element absolute value (white=zero). Evolutionary simulation parameters are: sum-rule mutation size $\mathcal{N}(0,0.05)$, product-rule mutation size $\mathcal{N}(1,0.27)$, $p = 0.0031$, tournament selection $s = 4$.

Fig. 4 - Escape from a fitness plateau entails a temporary decrease in modularity. Mean distance from maximal fitness as a function of time in the nonlinear model with product-rule mutations, towards a diagonal goal. Note the plateau in the dynamics. Matrices and their modularity drawn from the simulations at different time-points (designated by black points) are shown, with gray scale corresponding to element absolute value (white=zero). Inset: mean modularity of population (red curve), showing a sharp decrease at the time of escape from the plateau (same time points are shown). In order to escape the plateau (“break point”), the circled terms in A and B are changed. This occurs through a simultaneous increase of the new term and decrease of the old one, such that temporarily modularity is decreased (see inset). Finally, the correct arrangement of terms is attained (“escape”) and modularity increases again.

Fig 5: Time to high fitness and modularity grows polynomially with dimension. (A) Normalized distance to maximal fitness $|F|/(|G| + |AB|)$ as a function of generations in the nonlinear model evolved towards $G = 2I$, for matrix dimensions $D = 3$ to 10. Each color represents a different value of D . Curves typically have D “steps”, where each step corresponds to the build-up of an additional significant term. **(B)** Modularity in the same simulations. **(C)** Median time (generations) to high fitness (distance from maximal fitness < 0.01) as a function of the dimensions of the matrices D goes as $T \sim D^{\theta_1}$ with $\theta_1 = 1.41$ [1.40, 1.42] [CI 5%, 95%]. **(D)** Median time (generations) to modular structure (see methods for dimension dependent criterion for high modularity) goes as D^{θ_2} with $\theta_2 = 1.20$ [1.16, 1.23]. Initial conditions are random matrices with small elements drawn from $\mathcal{U}(0,0.1)$. Element-wise mutation rate p at all simulations was 0.0005; product-rule mutations normally distributed $\mathcal{N}(1,0.1)$. See SI Appendix for details on error calculation in C-D.

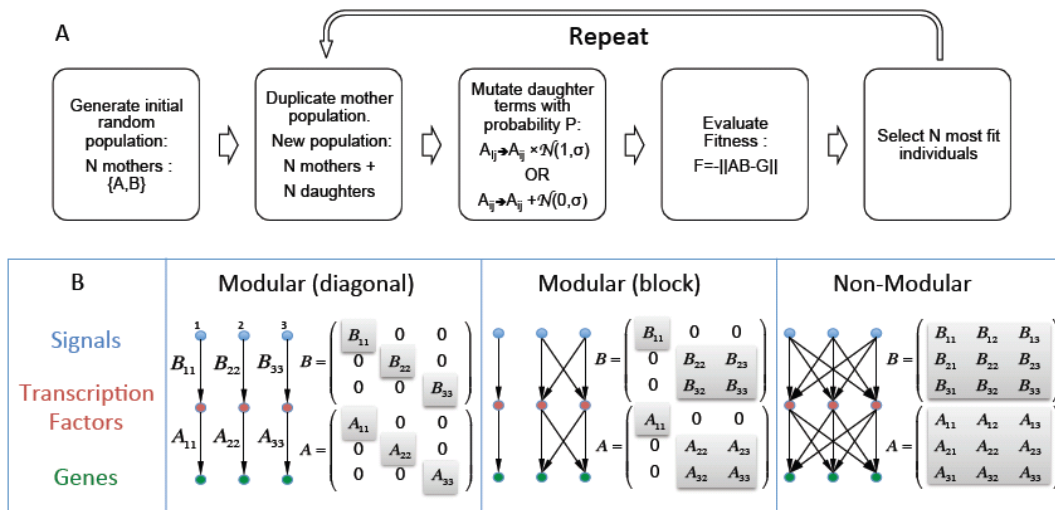


Fig. 1

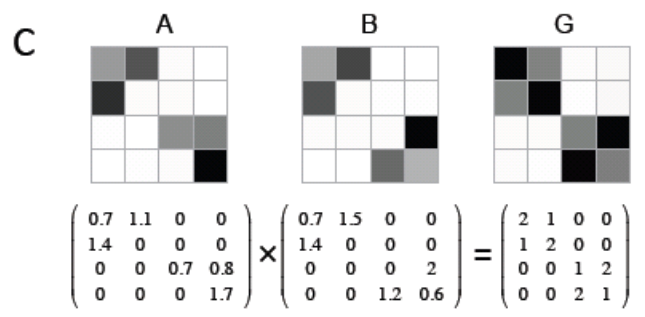
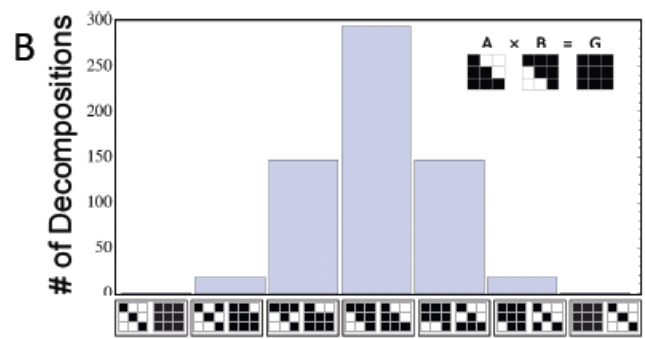
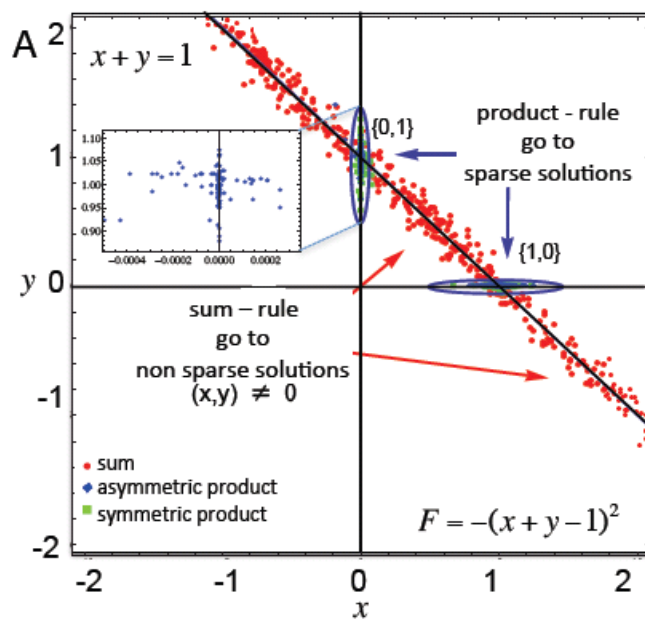


Fig. 2

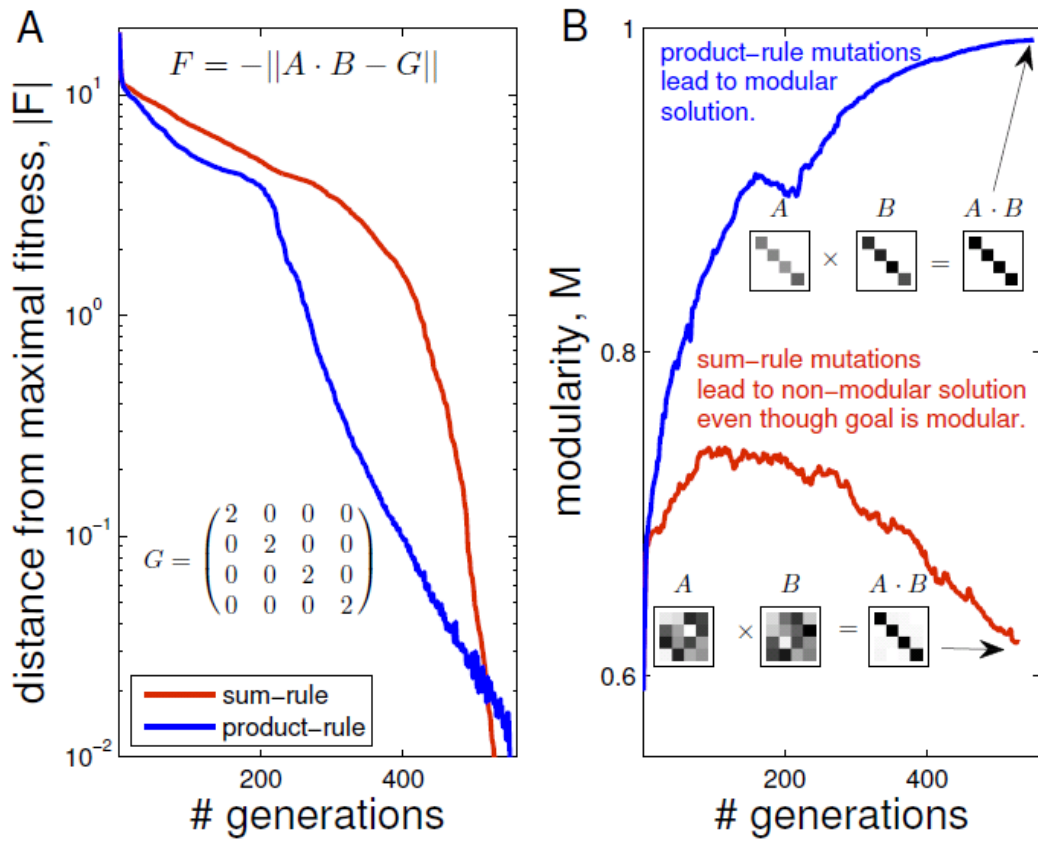


Fig. 3

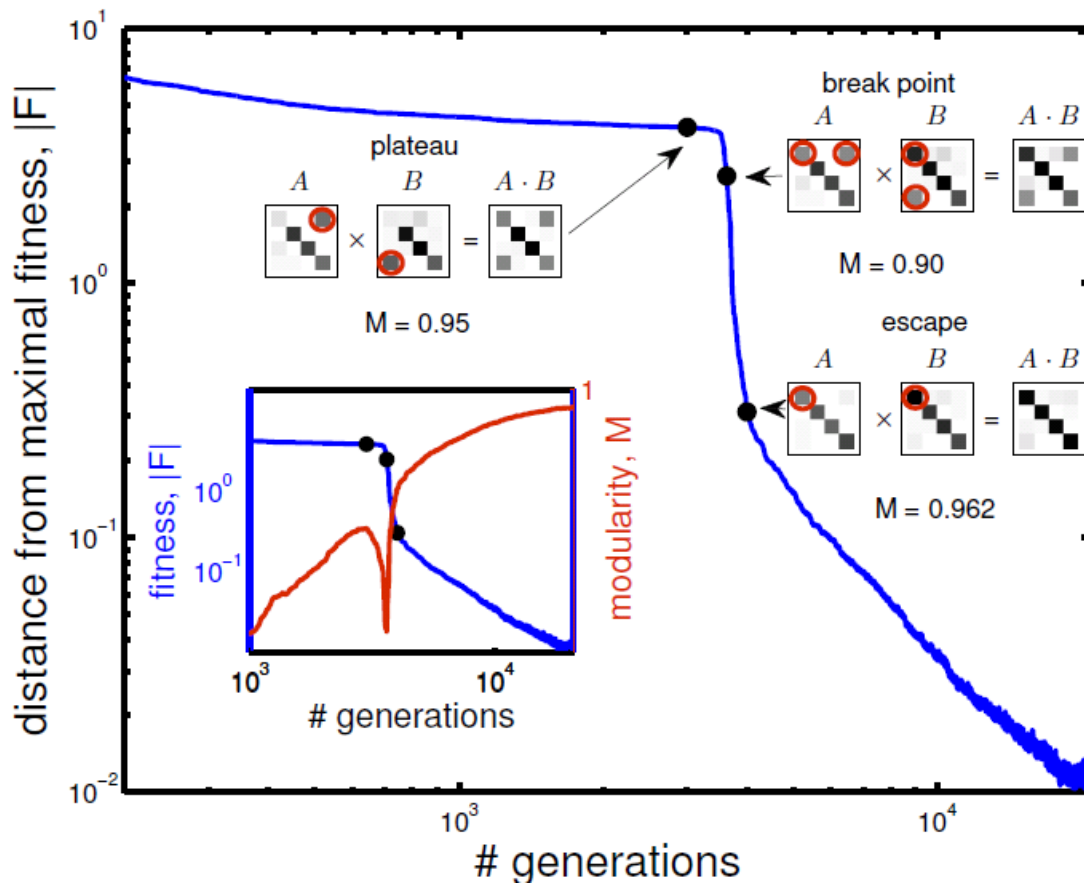


Fig. 4

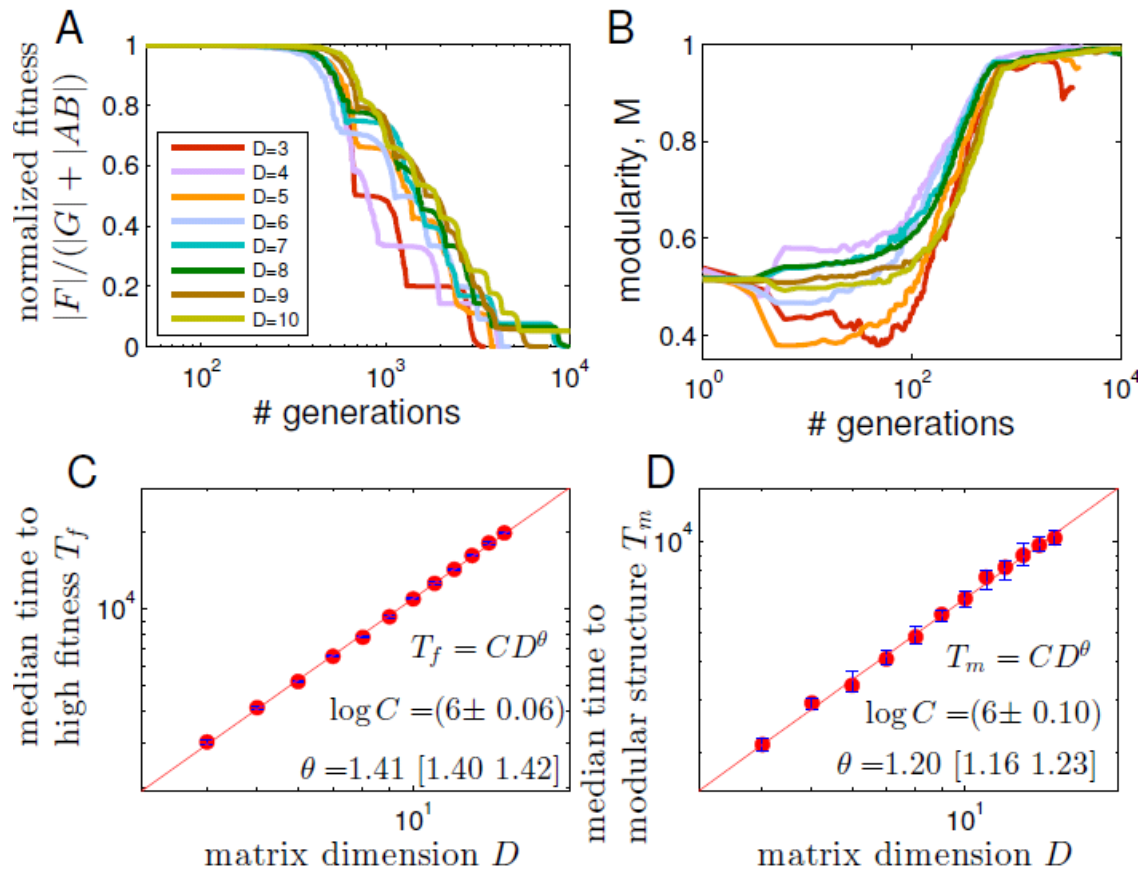


Fig. 5

Mutation Rules and the Evolution of Sparseness and Modularity in Biological Systems

Tamar Friedlander, Avraham E. Mayo, Tsvi Tlusty and Uri Alon

Supporting Information

Table of Contents

1. Analytical solution and simulations of toy model	22
2. Evolutionary simulations	32
3. Evolutionary Simulation Parameter Sensitivity test	34
4. Modularity: definitions and error calculation	36
5. LU decomposition - proofs	37
6. Nearly modular G	39
7. Mutation sign and distribution – supplementary figures.....	40

1. Analytical solution and simulations of toy model

To gain better insight into the effect of the product mutational mechanism we studied a simple toy model. We show that the effect of sum-mutations is equivalent to free diffusion in isotropic medium along equal fitness lines with no preference to any specific solution. Product-mutations in contrast are described by such diffusion in the log-transformed parameter domain, whereas in the non log-transformed domain they are log-normally distributed and asymptotically approach zero.

In our toy model the population exists in a 2-variable space and its goal is to reach the line where $x + y = 1$. All points on this line are equally fit, but only two of them - the intersections with the axes (0,1) and (1,0) are sparse (because one variable is zero). Fitness is evaluated by the square distance from this line, namely $F(x,y) = -(x + y - 1)^2$.

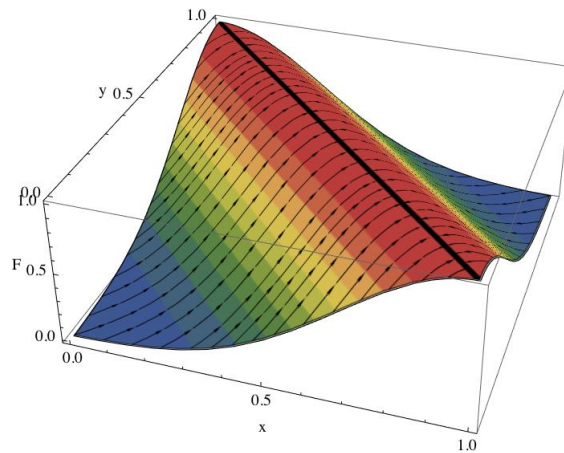


Fig S1: Decomposition of the x,y problem. Color represents fitness. Along equal fitness lines only mutation (diffusion) plays a role. Arrows show the other axis along which both selection and mutation are active. The maximal fitness line $x + y = 1$ is shown in bold.

The population dynamics is naturally decomposed into two axes: along equal-fitness lines dynamics is mutation (diffusion) dominated; in perpendicular to such lines it is determined by a combination of mutation and selection. We solve analytically the dynamics of the diffusion-dominated axis, and quantify the speed with which sparse solutions are approached with product-mutations. We also obtain a steady-state solution for the mutation-selection axis, showing that it obeys a Boltzmann distribution. We demonstrate our findings by detailed stochastic simulations (see below), showing excellent agreement with the analytical solutions.

Dynamics under sum-rule mutation

The mutation-selection dynamics of the population is approximately captured by the Fokker-Planck (FP) equation (1) in the limit of a large population and continuous time. We denote by

$P(x, y, t)$ the population distribution at time t . It is subject to the potential $F(x, y) = -(x + y - 1)^2$ (selection), and diffusion with coefficient D (mutation):

$$\partial_t P(x, y, t) = D \nabla^2 P(x, y, t) - \nabla \cdot (P(x, y, t) \nabla F(x, y))$$

This equation is the continuous approximation of the master equation describing the dynamics of a population living on a grid

$$P(x, t + \Delta t) = P(x, t) + \sum_z w(z, x) P(y, t) - \sum_z w(x, z) P(x, t)$$

where $w(z, x)$ is the transition probability from z to x . We further assume that transition is possible only between close grid points (i.e., mutations have a small effect). This translates to w being a narrow function of its arguments. Another assumption we make is that the transition probability depends on the difference in fitness between x and $x + \Delta x$. For example $w(x + \Delta x, x) = e^{(F(x+\Delta x)-F(x))}$. With this we get:

$$P(x, t + \Delta t) = P(x, t) + e^{(F(x+\Delta x)-F(x))} P(x + \Delta x, t) + e^{(F(x-\Delta x)-F(x))} P(x - \Delta x, t) - (e^{(F(x)-F(x+\Delta x))} + e^{(F(x)-F(x-\Delta x))}) P(x, t)$$

Expanding this equation to first order in Δt and second order in Δx , and rearranging we obtain the Fokker-Planck type equation as above with the diffusion coefficient D given by $\Delta x^2 / \Delta t$ as usual.

Taking into account the specific form of the fitness function F , it is convenient to make the following coordinate transformation:

$$u = x + y$$

$$v = x - y$$

With that, the potential and the FP equation transform to:

$$\tilde{F}(u) = -(u - 1)^2$$

$$\partial_t \tilde{P}(u, v, t) = 2D \partial_u \partial_u \tilde{P} + 2D \partial_v \partial_v \tilde{P} - \partial_u \tilde{F} \partial_u \tilde{P} - \tilde{P} \partial_u \partial_u \tilde{F}$$

This equation can be solved by separation of variables. We assume that the population already converged to the line of optimal fitness, $u = 1$. Therefore the time dependence of P enters only through $\tilde{P}(u, v, t) = V(v, t)U(u)$. The equation then reads:

$$\frac{\partial_t V - 2D \partial_v \partial_v V}{V} = \frac{2D \partial_u \partial_u U - \partial_u \tilde{F} \partial_u U - U \partial_u \partial_u \tilde{F}}{U} = \alpha = \text{const.}$$

For $\alpha \neq 0$ the equation in V describes a population growing with rate α . In our simulations we keep the population size constant, thus we set here $\alpha = 0$, and obtain the following equations for $U(u)$ and $V(v, t)$:

$$\partial_t V - 2D \partial_v \partial_v V = 0$$

$$2D \partial_u \partial_u U - \partial_u \tilde{F} \partial_u U - U \partial_u \partial_u \tilde{F} = 0$$

Thus, the dynamics of the V component is described by the diffusion equation with diffusion coefficient $2 \cdot D$. Its solution is the normal distribution with variance growing linearly in time (1, 2):

$$V(v, t) = \frac{1}{\sqrt{8\pi Dt}} e^{-\frac{v^2}{8Dt}}.$$

The solution for the U component is the Boltzmann distribution with potential F and effective 'temperature' D (1):

$$U(u) = \frac{e^{F(u)/D}}{\int e^{F(u)/D}}.$$

This steady state solution manifests the balance between selection and mutation by the ratio F/D. A low (high) F/D ratio results in a wide (narrow) distribution around the line of maximal fitness. In summary, along characteristics perpendicular to the optimal fitness line, the population density decays with the distance from the maximal fitness line; along characteristics parallel to this line the population diffuses freely. Our conclusions apply to any potential of the form $\tilde{F}(u) = g[(u - 1)^2]$. In the simulations, we used a specific function (see below).

This behavior is demonstrated in Figs. S2-S4, showing the distributions of $x + y$ and $x - y$ and the time-dependence of their moments obtained in simulations with sum-mutations.

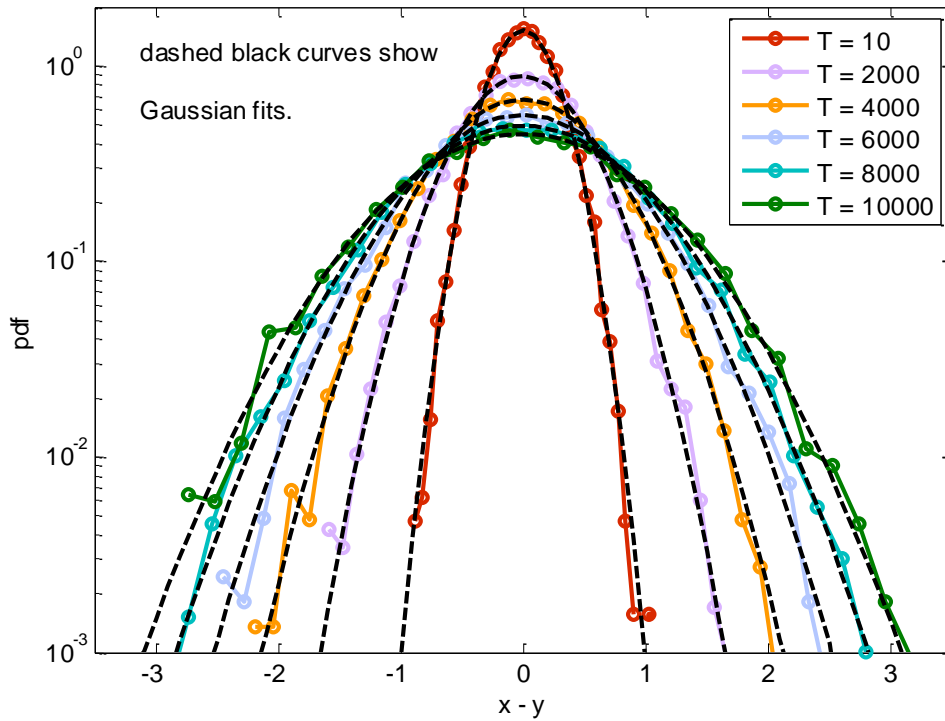


Fig S2: $x - y$ values with sum mutations are normally distributed in the x, y problem - simulation results. Colored solid curves illustrate distributions of $x - y$ values at different time points. Dashed black curves show best fit (in terms of maximal likelihood) to Gaussian - with excellent agreement. Time T is given in simulation number of generations. Simulation parameters: β - selection with $\beta = 5$, mutation normally distributed $N(0,0.05)$. Population was initiated at the origin. Results based on 10,000 points.

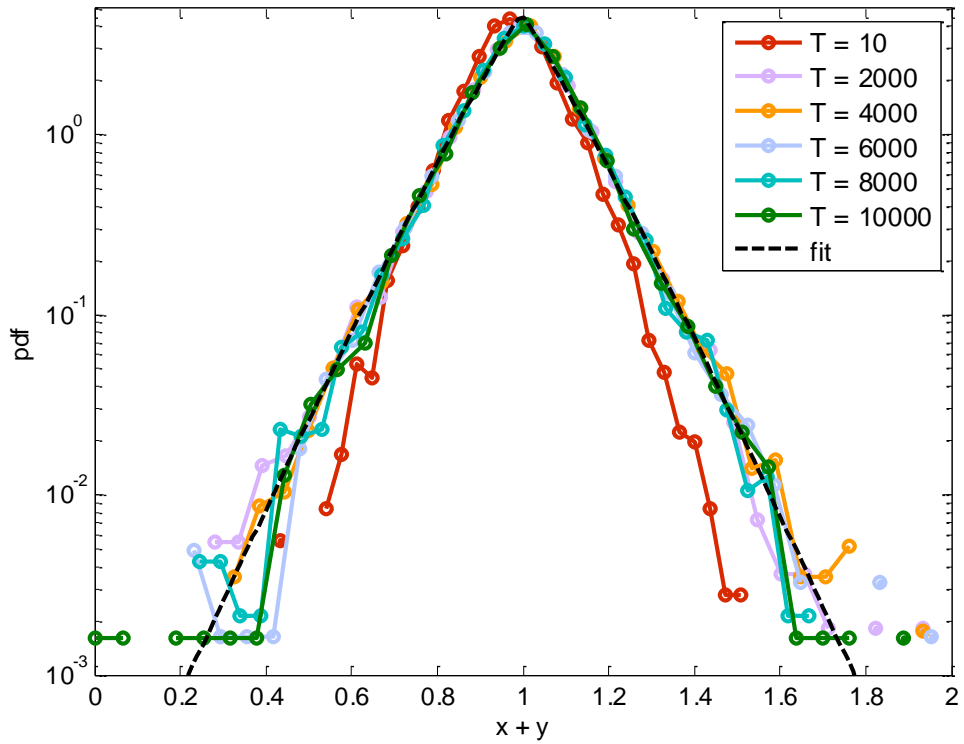


Fig S3: $x + y$ distributions with sum mutations converge to a stretched exponential distribution - simulation results. Colored solid curves illustrate distributions of $x + y$ values at different time points. Dashed black curve is fit to an effective potential $a \cdot e^{-b|x+y-1|^c}$ with $a=4.6$, $b=11.1$, $c=1$. All simulation points from $t = 5000$ were pooled together to produce the fit. Results pertain to the same simulations as in the previous figure.

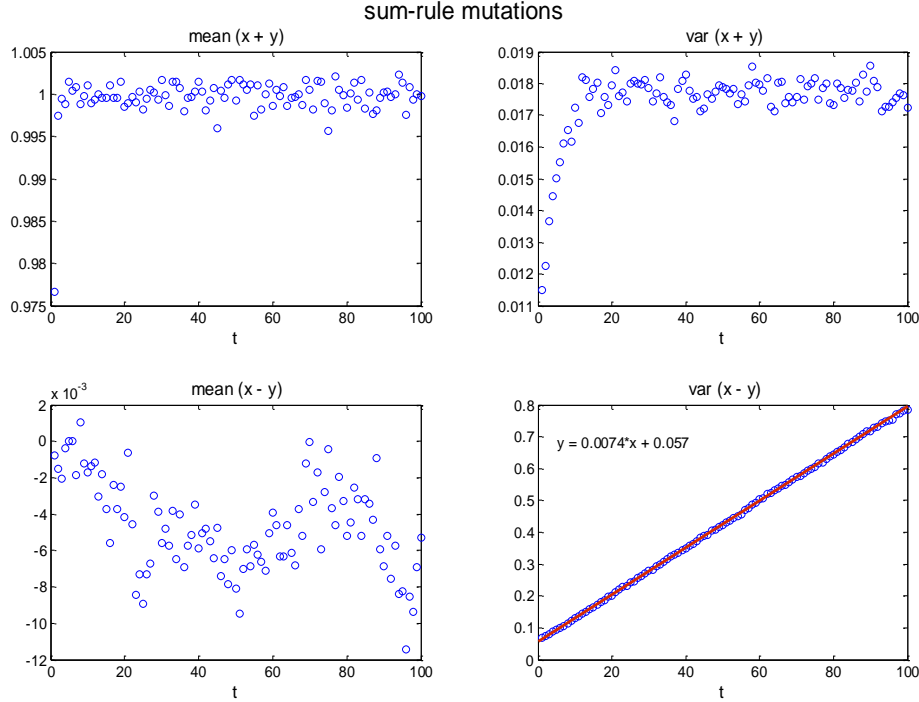


Fig S4: Mean and variance time-dependence of $x + y$ and $x - y$ in sum-rule simulations show decomposition into two functional axes. Selection rapidly drives the $x + y$ component to converge to the line $x + y = 1$ with constant variance. In contrast, the $x - y$ component freely diffuses, exhibiting a variance that grows linearly in time, in accordance with the analytical solution. The red line is a linear fit. Time t is given in thousands of simulation generations.

Dynamics under product-rule mutation near the sparse solution (0,1)

We now turn to product-rule mutations. In the log-transformed domain, the FP equation incorporates diffusion with constant coefficient, solvable similarly to the sum-mutation case. Once a solution is found in the log-transformed domain, one can transform it back to the original variables. We use this indirect way, rather than writing the equation directly, because the FP equation is a second order approximation of the general master equation assuming localized transitions. However, this locality assumption breaks down because of the exponential form of the transformation. Without loss of generality, we concentrate here on one of the two sparse solutions (0,1).

Using the transformation:

$$x = e^{G_x}$$

$$y = e^{G_y}$$

where G_x and G_y are the log-transformed variables of x and y respectively. The fitness function F (the potential in the FP equation) is:

$$F(G_x, G_y) = -(e^{G_x} + e^{G_y} - 1)^2.$$

The sparse solution is obtained in the limit $(G_x, G_y) \rightarrow (-\infty, 0)$. The asymptotic form of the fitness in this limit again depends only on one of the variables

$$F(G_x, G_y) \rightarrow -(e^{G_y} - 1)^2.$$

With this in mind, the FP equation in log-transformed variables is:

$$\partial_t P = D \partial_{G_x} \partial_{G_x} P + D \partial_{G_y} \partial_{G_y} P - \partial_{G_y} (P \partial_{G_y} F(G_y)).$$

Using similar reasoning as in the sum-mutation case, we substitute $P = X(G_x, t)Y(G_y)$:

$$\partial_t X - D \partial_{G_x} \partial_{G_x} X = 0$$

$$D \partial_{G_y} \partial_{G_y} Y - \partial_{G_y} (Y \partial_{G_y} F(G_y)) = 0$$

The solution for the Y component is as before:

$$Y(G_y) = \frac{e^{F(G_y)/D}}{\int e^{F(G_y)/D}} \rightarrow \tilde{Y}(y) = \frac{e^{F(y)/D}}{\int e^{F(y)/D}},$$

which means that the population is concentrated around $e^{G_y} = y = 1$ with variance D . The solution for the X component is again a Gaussian with variance that grows linearly in time:

$$X(G_x, t) = \frac{1}{\sqrt{4\pi Dt}} e^{-\frac{G_x^2}{4Dt}}.$$

Transforming to the original variables we find:

$$X(G_x, t) dG_x = \tilde{X}(\log(x), t) \frac{dx}{x}$$

or

$$\tilde{X}(t, x) dx = \frac{1}{x\sqrt{4\pi Dt}} e^{-\frac{[\log(x)]^2}{4Dt}} dx.$$

This is a lognormal distribution (3) with mode (most probable value) that converges to zero like $\exp(-2D t)$, but mean that diverges like $\exp(D t)$. For large t , the leading term in the asymptotic expansion of this distribution goes like $\sim \frac{\sqrt{1/t}}{x\sqrt{4\pi D}}$.

Simulation results demonstrating this behavior are shown in Figs. S5-S7.

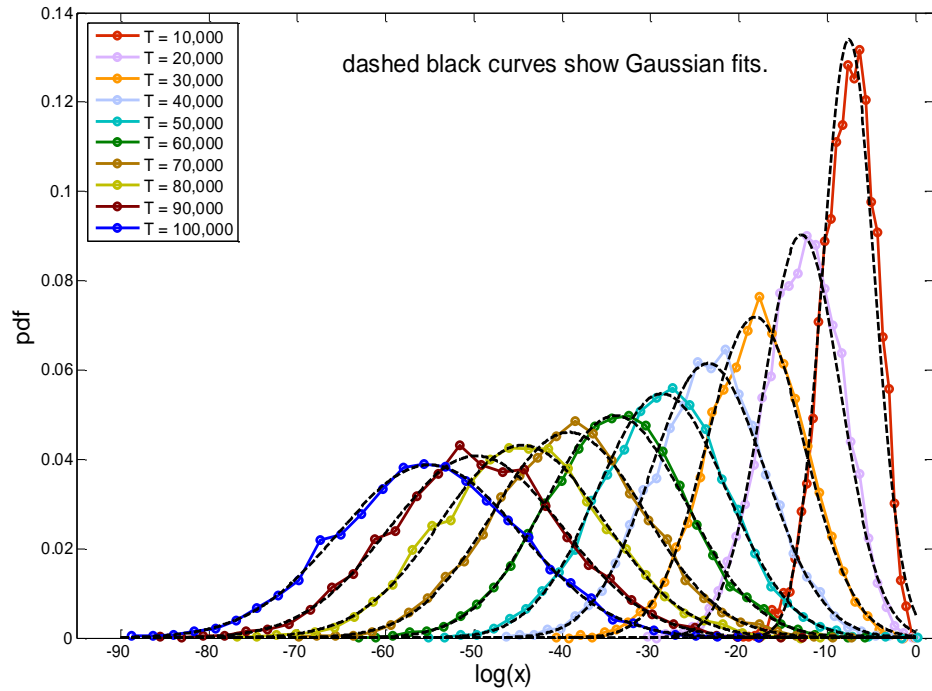


Fig S5: x values with product mutations are log-normally distributed and asymptotically approach zero in the x, y problem - simulation results. Colored solid curves illustrate distributions of $\log(x)$ values at different time points. Dashed black curves show best fit (in terms of maximum likelihood) to Gaussian – with excellent agreement. Time T is given is simulation number of generations. Simulation parameters: β -selection with $\beta = 5$, mutation normally distributed $N(1,0.2)$. Population was initiated at the origin. To concentrate on one of the two sparse solutions, only simulation points with $0 < x < 0.5$ were considered in this analysis (roughly ~ 6000 points at each time point).

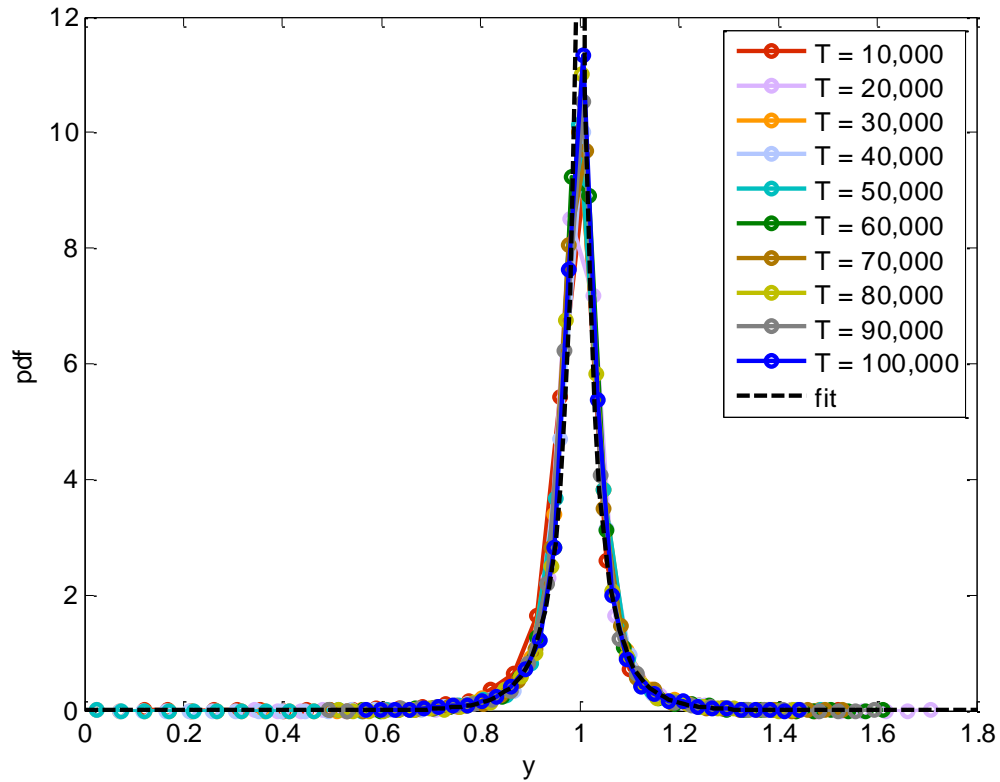


Fig S6: y values with product mutations converge to a stretched exponential distribution - simulation results. Colored solid curves illustrate distributions of y values at different time points. Dashed black curve shows fit to an effective potential $a \cdot e^{-b|y-1|^c}$ with $a=21.19$, $b=14.8$, $c=0.67$. Time T is number of generations. Results pertain to the same simulation points as in the previous figure (i.e. the y values corresponding to $0 < x < 0.5$).

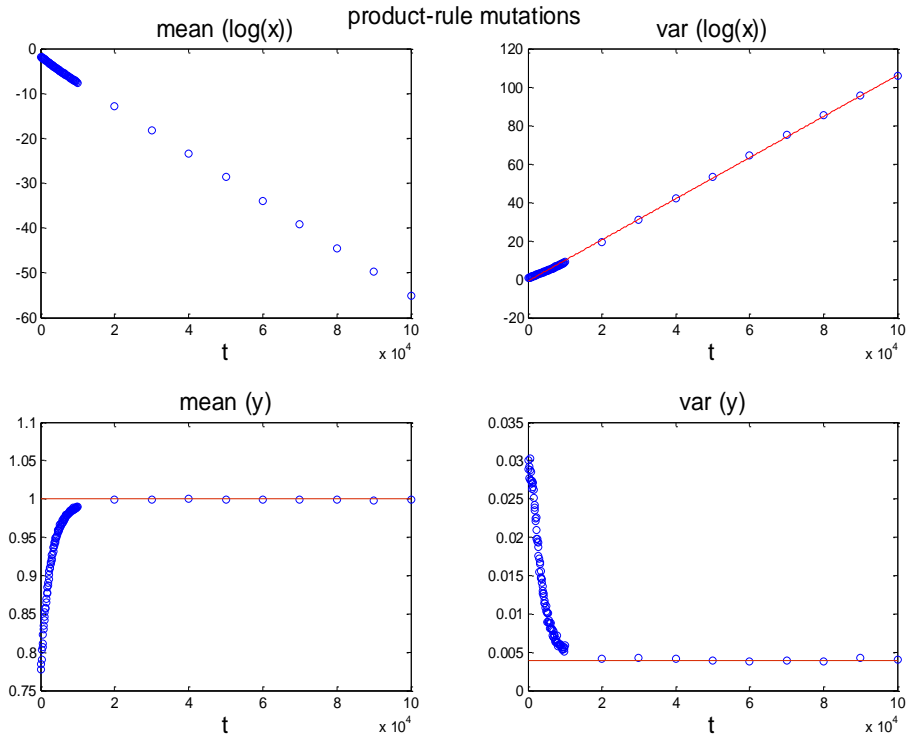


Fig S7: Time dependence of x moments under product-rule mutations agrees with log-normal distribution predicted by analytical solution – simulation results. Time variance of $\log(x)$ is found to grow linearly in time and mean of $\log(x)$ decreases linearly, as expected if there is free diffusion in the log-transformed variable. Top row: red lines show best linear fits. In contrast, both the mean and the variance of y converge to a constant (red lines were added to guide the eye). Results pertain to the same simulations as in the previous figure.

Stochastic simulations of toy model

To estimate the temporal behavior of population distributions in this toy model we performed repeated runs of our simulation. At each run we randomly sampled a single individual from the population at the sampled time point. This was done in order to avoid dependence between different population members at the same population, stemming from finite population size. Each run was initiated with a different random seed, to assure independence of the distinct runs. Simulation consisted of repeated mutation-selection rounds, as described in the Methods section of the main text. We used β -selection with $\beta = 5$. Mutations were normally distributed $N(0,0.05)$ for sum rule mutations and $N(1,0.2)$ for product rule mutations. Simulation was initiated with the population normally distributed around the origin $x = 0, y = 0$, with std 0.1 in both x and y axes.

The β -selection includes fitness scaling of the form: $f_i \rightarrow \frac{e^{-\beta(x_i+y_i-1)^2}}{\sum_i e^{-\beta(x_i+y_i-1)^2}}$. However, the relation to the potential is more complicated. Thus, we fit the simulation results to an effective potential of the form $b \cdot |x + y - 1|^c$.

Under these initial conditions the product-rule mutations have equal probability to converge to either one of the two sparse solutions. Simulation results are thus a superposition of the two solutions. When relevant to the analysis, we separated simulation points. To show the distribution approaching to the (0,1) solution we selected only points with $x < 0.5$.

To plot distributions of product-mutation simulation we used uniform binning in the log domain. Fits to Gaussian are maximum likelihood estimators under the assumption that the data is normally distributed, calculated using the Matlab function 'normfit'.

2. Evolutionary simulations

Here we detail our evolutionary simulations. Simulations were in Matlab using a standard framework (4, 5). We initialized the population of matrix pairs by drawing their $N \cdot 2D^2$ terms from a uniform distribution at either small range, i.e. $\mathcal{U}[0, 0.1]$ or large range $\mathcal{U}[0,1]$ - where small and large are compared to the largest elements in the goal matrix (which are of order one). In other simulations we used initial values drawn from a normal distribution around zero with std 0.1 or 1. Most results shown refer to the small range, which relates to evolution of a structure with only weak initial interactions; however our conclusions apply also to the large range. Population size was set to $N = 500$.

At each generation the population was duplicated. One of the copies was kept unchanged, and elements of the other copy had a probability p to be mutated – as we explain below. We note that it is also common to keep a single copy of the population and mutate it. The former technique is less likely to lose a good solution once it is found, but its convergence is relatively slow, whereas the latter technique is faster, but might lose beneficial solutions that have already been found (see discussion in (4) chap. 10). Fitness of all $2N$ individuals was evaluated by $F = -||AB - G||$, where $|| \cdot ||$ denotes the sum of squares of elements (Frobenius norm). This formula represents the Euclid distance of the matrix product from the goal (6). The best possible fitness here is zero, achieved if $AB = G$ exactly. Otherwise, fitness values are negative. In the figures we usually show the absolute value of mean population fitness. The goal matrix was either diagonal $G = 2 \times I$, nearly-diagonal (diagonal matrix with small non-diagonal terms), block-diagonal or full rank with no zero elements. N individuals were then selected out of the $2N$ population of original and mutated ones, based on their fitness. This mutation–selection process was repeated again and again until the simulation stopping condition was satisfied (usually when mean population fitness was less than 0.01 from the optimum).

Mutation: We tested point mutations in our simulation and assumed statistical independence between mutations at different elements. We kept mutation rate such that on average 10% of the population members were mutated at each generation, so the element-wise mutation rate p for matrices of dimension D was at most $\frac{0.1}{2D^2}$. This relatively low mutation rate enables beneficial mutants to reproduce on average at least 10 times before they are mutated again. In simulations where we compared dependence on matrix dimension (Fig. 5) we used the same mutation rate at all dimensions, generally the one that pertains to the highest dimension used in the simulation.

We randomly picked the matrix elements (in both A and B) that would be mutated. Mutation values were drawn from a Gaussian (or log-normal or Gamma) distribution. For sum-rule mutation, this random number was added to the mutated matrix value: $A_{ij} \rightarrow A_{ij} + \mathcal{N}(0, \sigma)$ or $B_{ij} \rightarrow B_{ij} + \mathcal{N}(0, \sigma)$, and for product-rule, the mutated matrix element was multiplied by the random number: $A_{ij} \rightarrow A_{ij} \cdot \mathcal{N}(\mu, \sigma)$ or $B_{ij} \rightarrow B_{ij} \cdot \mathcal{N}(\mu, \sigma)$. Mean mutation value μ was usually taken as 1, however we also tested other values of μ (both larger and smaller than 1) and results remained qualitatively similar, only the time-scales changed. We also tested the dependence on the mutation size σ , using $\sigma = 0.01 - 3$, and found similar results. In most simulation results shown here we used $\sigma = 0.1$ (unless stated otherwise). Fitness convergence crucially depends on the mutation frequency and size, as demonstrated in our sensitivity test. Grossly speaking, a high mutation rate can speed up evolution at the beginning of the simulation, but can later on preclude slightly better mutants from taking over, because they are mutated again before they reproduce sufficiently. There is also a similar trade-off with mutation size: large mutations can speed evolution at the beginning, but at the final stages the mutation size limits the precision with which the goal can be approached.

Selection methods: We tested 3 different selection methods; all gave qualitatively very similar results with only difference in time scales. Most results presented here were obtained with tournament selection (see (4) chap. 9): N sets, each containing s population members, were uniformly drawn with repetitions. The best individual at each set was then selected to be at the population next generation. This mimics the fact that an individual needs to outperform only others at its close vicinity, rather than the whole population. The parameter s can be used to tune the selection intensity (the larger it is, the stronger is the selection). In our simulations we set $s = 4$.

Another selection method tested is “truncation-selection” or “elitism”. Here population members were ranked by their fitness. The best half of members were selected and duplicated. We note that both methods are based on the fitness rank, rather than on its exact value, making fitness scaling unnecessary. Both methods gave very similar results.

The third method used was proportionate reproduction with Boltzmann-like scaling (7–9): here the relative fitness was computed as $\tilde{F}_i = e^{\beta F_i} / \sum_j e^{\beta F_j}$. Evidently $\sum_j \tilde{F}_i = 1$, so that \tilde{F}_i is the probability of the i -th individual to be selected. The parameter β determines the selection

strength, where at one extreme if $\beta = 0$, all individuals are equally probable to be selected and at the other extreme if $\beta = \infty$, the best individual is selected with probability 1, while all others have probability zero to be selected. To implement selection we then exploited the “roulette-wheel” algorithm (4, 5) where a section of the interval $[0,1]$ equal to \tilde{F}_i was assigned to the i -th individual. N Random numbers were then uniformly drawn from the interval $[0,1]$. The individuals whose sections contained such numbers were then selected (with repetitions).

For a comparative test of the dependence of fitness achieved and the time needed to reach it on selection and mutation parameters see sensitivity test below.

If selection is too weak (e.g. $\beta = 0.1$ in Boltzmann-like selection) sparse structures are obtained, but their fitness is far from optimal. If the fraction of individuals mutated at each generation is too high (e.g. every individual has on average one mutation per generation), then again the solutions obtained are bounded away from the optimum, because high fitness individuals are likely to suffer from additional deleterious mutation before they reproduce sufficiently.

3. Evolutionary Simulation Parameter Sensitivity test

Here we show in Fig. S8 the dependence on mutation size and selection intensity β of the evolutionary simulation with the Boltzmann-like selection scheme. In this test we let the simulation solve a 1-D problem for a fixed number of generations (=800), with a single repeat for each parameter combination. We tested 6 different values of β (0.1-20) and 5 different values of the mutation size σ (0.01-0.5). Here we plot either the mean population fitness (top row: **A** and **B**) or the best fitness obtained within the population (bottom row: **C** and **D**), reached within this fixed number of generations. In the left panels (**A** and **C**) each curve illustrates the dependence on β for a fixed mutation size, and the right panels (**B** and **D**) show the dependence on mutation size where each curve was obtained for a different values of β . Curves in both left and right panels were created by the same simulation results.

Alternatively, we tested how the time to reach a desired fitness (0.01 from the optimum) depends on these parameters in a 3-D problem. The number of generations was limited to 500,000 and some parameter combinations failed to reach the required fitness by that time. Similarly, we show in Fig. S9 the dependence on β for fixed mutation size (**A**) or dependence on mutation size for fixed β (**B**).

Based on these tests we chose to set the mutation size $\sigma = 0.1$ and the selection intensity $\beta = 10$ (Boltzmann-like) or $s = 4$ (tournament).

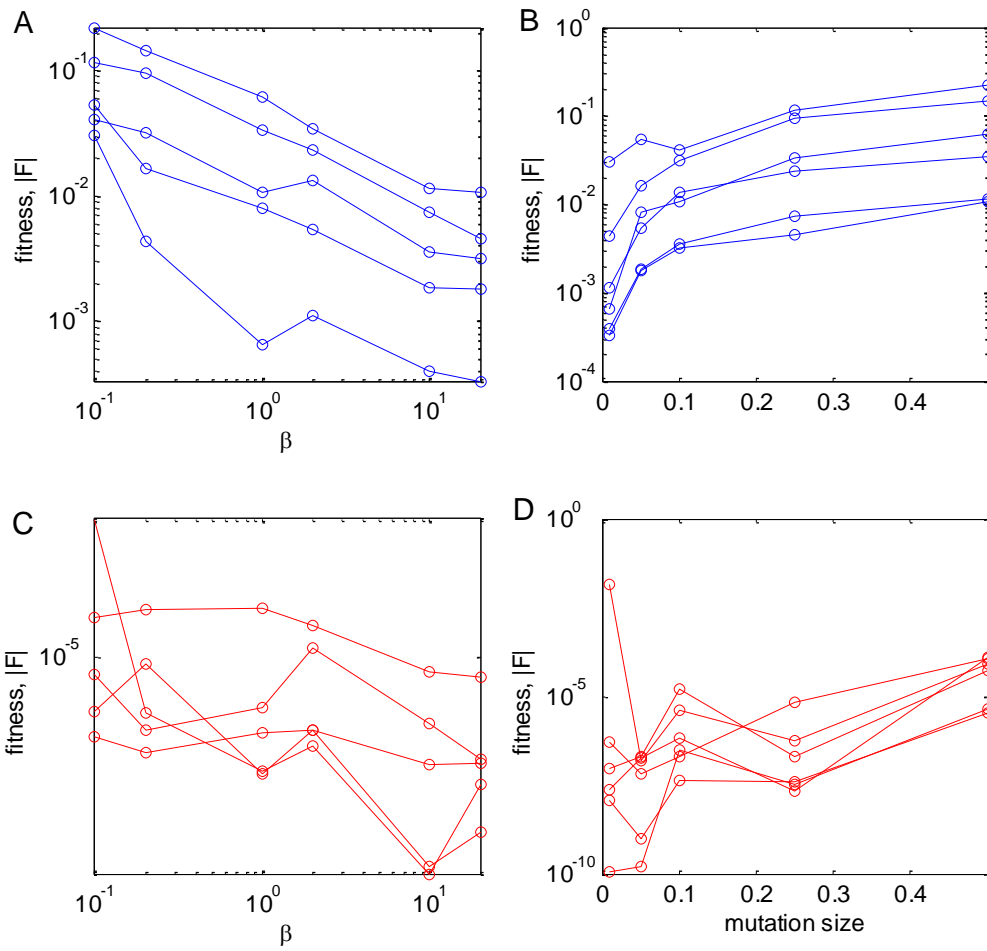


Fig S8: Dependence of the achieved fitness on selection strength and mutation size in a 1-D problem.

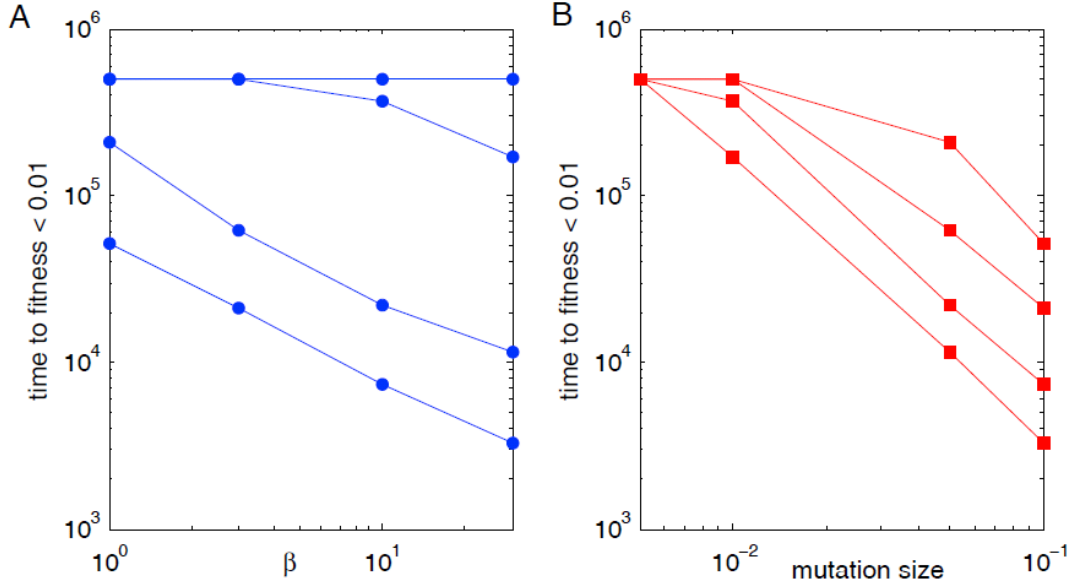


Fig S9: dependence of the time to reach a desired fitness value on selection strength and mutation size.

4. Modularity: definitions and error calculation

Definition of modularity: if the goal is diagonal, we define modularity as $M = 1 - \langle |n| \rangle / \langle |d| \rangle$ where $\langle |n| \rangle$ and $\langle |d| \rangle$ are the mean absolute value of the non-diagonal and diagonal terms respectively. At each generation, the D largest elements of each matrix (both A and B), were considered as the diagonal $\langle |d| \rangle$ and the rest $D^2 - D$ terms as the non-diagonal ones $\langle |n| \rangle$. Averages were taken over matrix elements and over the population. This technique copes with the unknown location of the dominant terms in the matrices, which could form any permutation of a diagonal matrix. Thus, $0 \leq M \leq 1$: where at the two extremes, a diagonal matrix has $M = 1$, and a matrix with equal terms has $M = 0$. Since we choose the largest elements to form the diagonal, negative values of M are not allowed. When the goal is non-diagonal, one can use standard measures for modularity such as (10).

Calculation of time to modularity: we used the following approximation for fitness value when the goal is diagonal. Assume that A and B are D -dimensional matrices consisting of 2 types of terms: diagonal terms all with size d and non-diagonal terms all with size n and that the goal is $G = g \times I_{D \times D}$. The fitness then equals:

$$-F = D[d^2 + (D - 1)n^2 - g]^2 + D(D - 1)(2dn + (D - 2)n^2)^2.$$

We collect terms by powers of n , and obtain a constant term and terms with powers $n^{2,3,4}$. Modularity is obtained when the solution has the correct number of dominant terms appropriately located and their size is approximately $d^2 \cong g$. At the beginning of the temporal

trajectory, when non-diagonal elements are relatively large, F is dominated by the $O(n^4)$ term. When a modular structure emerges, non-diagonal elements become relatively small, and the dominant term remaining in F is $O(n^2)$. Our criterion for determining time to modularity was the time when the n^2 term first became dominant, i.e. when $F - n^2(\dots) < n^2(\dots)$.

Matrix permutations: For ease of presentation we permuted the A and B matrices, so that they form nearly-diagonal matrices. This applies to the cases when G is diagonal and A and B also evolve to be (nearly) diagonal. We used the same permutation for the rows of A and columns of B . Such permutation preserves the matrix product and is equivalent to simply changing the order of inputs. To find the correct permutation, we sorted each column of A in descending order. Then the first row in the sorted matrix had the D largest elements. We used the order vector of this first row (i.e. indices of rows where these elements were located in the original A) as the required permutation.

Calculation of error bars in time dependence on D : We repeated the simulation at each dimension either $K = 140$ times ($D = 3 - 10$) or $K = 80$ times ($D = 11 - 15$), initializing the Matlab random seed with a different integer number each time. At each run we measured time to reach fitness within 0.01 of the optimum and time to modularity, as explained above. As these times formed a broad and highly skewed distribution, we considered their median, rather than their mean. To estimate our error in this median estimator, we used the following bootstrapping procedure. We randomly formed sets of K samples (with repetitions) of simulation results. We constructed $L = 10,000$ such sets, and calculated the median of each. We then calculated the standard deviation of these median values. To estimate the error in the dependence of the time on D , we randomly picked one measurement from each dimension and then calculated the best line (in terms of least squares) connecting these points. We repeated this process 10,000 times, receiving each time different parameters for the best line. Errors in line estimation presented here, represent the 5% and 95% quantiles out of the obtained distribution of line parameters.

5. LU decomposition - proofs

An LU decomposition exists for every full rank matrix (11). In such decomposition there is a total of $D^2 - D$ zeros in both A and B together. Here we prove that a larger number of zeros is not possible unless G has a zero term (or is not full rank).

The $D^2 - D$ zeros can be partitioned between A and B in different ways: either equally (the LU decomposition, where A and B are triangular matrices), or all zeros in one of the matrices and none in the other or any other partition.

Theorem: maximal number of zeros in LU decomposition of a full rank matrix with no zero elements is $D^2 - D$.

Lemma: Let $A_1B_1 = G = A_2B_2$ be 2 different decompositions of the goal G with different zero partitions, such that all matrices are invertible. Then, there exists an invertible transformation matrix P , such that $A_1P = A_2$ and $P^{-1}B_1 = B_2$.

Proof: Define $P = (A_1)^{-1}A_2$. Then $A_1P = A_1(A_1)^{-1}A_2 = A_2$ and $P^{-1}B_1 = (A_2)^{-1}A_1B_1 = (A_2)^{-1}G = (A_2)^{-1}A_2B_2 = B_2$.

Q.E.D

If a transformation exists between all pairs of decompositions, specifically we can choose A_2B_2 in which A is full and B is diagonal, i.e. all $D^2 - D$ zeros are in B . Now let's check what happens if we try to add one more zero. Then, because B is diagonal, $G_{ij} = \sum_k A_{ik}B_{kj} = A_{ij}B_{jj}$, $\forall i, j$. Without loss of generality we set $A_{ij} = 0$, then essentially $G_{ij} = 0$, so G is not a general matrix.

Alternatively if we set $B_{jj} = 0$, we will obtain that the j -th column of G is all zeros – hence G is not full rank.

Q.E.D

Theorem: If G is full rank but has k zeros, the maximal number of zeros in LU decomposition is $D^2 - D + k$.

As stated above, for a general full rank G a decomposition in which A is full and B is diagonal, (i.e. there is a total of $D^2 - D$ zeros) is possible.

Now assume without loss of generality that $G_{ij} = 0$. Since B is diagonal $G_{ij} = A_{ij}B_{jj}$, so that A_{ij} must be zero too ($B_{jj} \neq 0$ because otherwise a full column in G equals zero and then G is not full rank). Consequently, for every zero in G , we obtain exactly one additional zero in A , which proves our claim that for G with k zeros, we obtain a decomposition with exactly $D^2 - D + k$ zeros.

Due to the lemma above, these zeros can be split in different ways between A and B .

Q.E.D

6. Nearly modular G

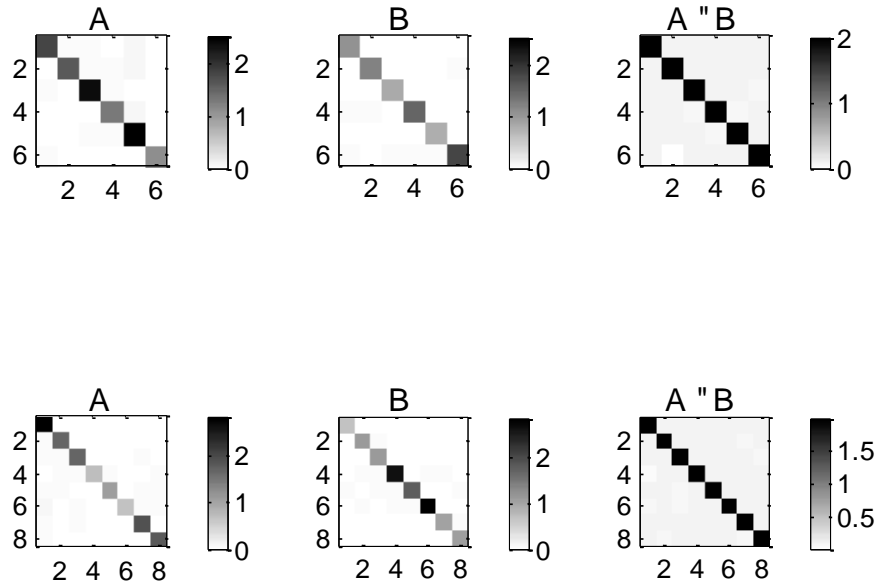


Fig S10: If the goal G is nearly diagonal, the evolutionary simulation reaches solutions in which A and B are nearly-diagonal too. We set G to be a matrix with values of 2 on its diagonal and 0.1 in its all non-diagonal terms. Here we show two examples of solutions obtained for $D = 6$ (top row) and $D = 8$ (bottom row). Numerical values are represented by color code when white represents zero. Matrices were permuted to form the most diagonal form (see above).

7. Mutation sign and distribution – supplementary figures

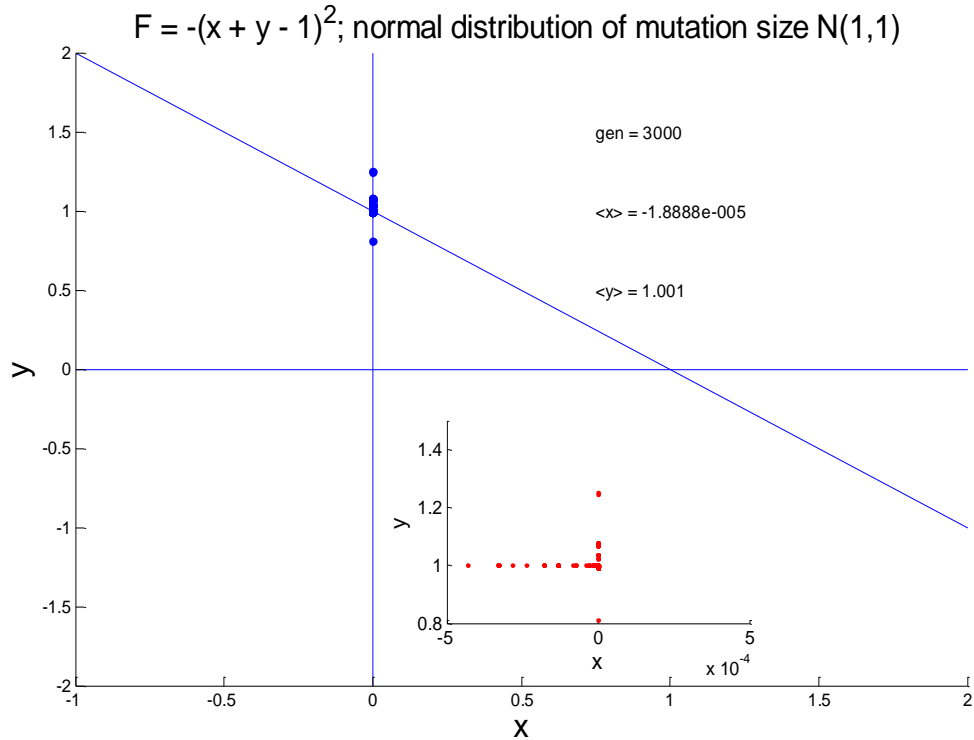


Fig S11: Broad distribution of mutation values allows for negative as well as positive matrix values. Here we show the distribution of solutions to the x, y problem with product mutations normally distributed $N(1,1)$. The solutions concentrate near the modular point $(0,1)$. Inset demonstrates that the x values are in fact negative in this case. Simulation was run for 3000 generations. Mean x and y values are written on top of the graph.

References

1. Gardiner C (2004) *Handbook of Stochastic Methods: for Physics, Chemistry and the Natural Sciences* (Springer). 3rd Ed.
2. Metzler R, Klafter J (2000) The random walk's guide to anomalous diffusion: a fractional dynamics approach. *Physics Reports* 339:1–77.
3. Limpert E, Stahel WA, Abbt M (2001) Log-normal distributions across the sciences: keys and clues. *BioScience* 51:341–352.
4. Spall JC (2003) *Introduction to Stochastic Search and Optimization: Estimation, Simulation and Control* (Wiley-Blackwell).

5. Goldberg DE (1989) *Genetic Algorithms in Search, Optimization, and Machine Learning* (Addison-Wesley).
6. Fisher RA (1930) *The Genetical Theory of Natural Selection* ed Bennett JH (Oxford University Press, USA). 1st Ed.
7. Burda Z, Krzywicki A, Martin OC, Zagorski M (2010) Distribution of essential interactions in model gene regulatory networks under mutation-selection balance. *Phys Rev E* 82:011908.
8. Lampert A, Tlustý T (2009) Mutability as an altruistic trait in finite asexual populations. *Journal of Theoretical Biology* 261:414–422.
9. Lipson H, Pollack JB, Suh NP (2007) On the origin of modular variation. *Evolution* 56:1549–1556.
10. Newman MEJ (2006) Modularity and community structure in networks. *Proceedings of the National Academy of Sciences* 103:8577–8582.
11. Cormen TH, Leiserson CE, Rivest RL, Stein C (2001) *Introduction To Algorithms* (MIT Press).

